

# Tunable band gap and optical properties of surface functionalized Sc<sub>2</sub>C monolayer\*

Shun Wang(王顺)<sup>1,2,3</sup>, Yu-Lei Du(杜宇雷)<sup>1,†</sup>, and Wen-He Liao(廖文和)<sup>1</sup>

<sup>1</sup>School of Mechanical Engineering, Nanjing University of Science and Technology, Nanjing 210094, China

<sup>2</sup>School of Materials Science and Engineering, Nanjing University of Science and Technology, Nanjing 210094, China

<sup>3</sup>School of Materials Science and Engineering, Henan University of Technology, Zhengzhou 450001, China

(Received 7 August 2016; revised manuscript received 8 September 2016; published online 30 November 2016)

Using the density functional theory, we have investigated the electronic and optical properties of two-dimensional Sc<sub>2</sub>C monolayer with OH, F, or O chemical groups. The electronic structures reveal that the functionalized Sc<sub>2</sub>C monolayers are semiconductors with a band gap of 0.44–1.55 eV. The band gap dependent optical parameters, like dielectric function, absorption coefficients, reflectivity, loss function, and refraction index were also calculated for photon energy up to 20 eV. At the low-energy region, each optical parameter shifts to red, and the peak increases obviously with the increase of the energy gap. Consequently, Sc<sub>2</sub>C monolayer with a tunable band gap by changing the type of surface chemical groups is a promising 2D material for optoelectronic devices.

**Keywords:** two-dimensional material, first-principles, band gap, optical properties

**PACS:** 78.67.–n, 73.20.At, 31.15.A–

**DOI:** 10.1088/1674-1056/26/1/017806

## 1. Introduction

*MXene*, a recently discovered family of two-dimensional (2D) transition metal carbides and nitrides, is receiving increasing emphasis due to its appealing opportunities for practical applications in energy storage systems, electronic devices, catalysts, and spintronics.<sup>[1,2]</sup> The synthesis of *MXene* is achieved from *MAX* phases by selective etching of the *A* layers, where *M* is an early transition metal, *A* is an element from groups 3 and 5, and *X* is C or N.<sup>[3,4]</sup> In the etching process with HF acid, weak interacting bare *MXene* is spontaneously passivated by the F, OH, or O termination groups (labeled as *T* groups) on both surfaces.<sup>[5,6]</sup> Although the functionalized *MXenes* are based on the same transition metal carbides and nitrides, they have completely distinct properties according to the type of *T* groups.<sup>[7–12]</sup> The previous theoretical researches have indicated that surface functionalization has a significant impact on the crystal structure and phase stability of *MXenes*.<sup>[7]</sup> Electronic, elastic, and thermal transport properties of *MXenes* are also strongly affected by surface functionalization.<sup>[8–10]</sup> Specific *MXenes* with excellent electron mobility and high thermal conductivity can be obtained by surface functionalization.<sup>[11,12]</sup> Therefore, understanding the effect of surface functionalization on the properties of *MXenes* is the foundation of practical applications for the new 2D materials.

Pristine *MXene* monolayers are commonly metallic without a band gap. Recent advances in band gap engineering of graphene have motivated the studies of tuning the band gap of 2D *MXenes*.<sup>[13–17]</sup> These investigations illuminate that the

properties of *MXenes* can be modified by surface functionalization and strain engineering. Some of the initially metallic *MXenes* become semiconductors with a small energy band gap by surface functionalization. Among these semiconducting *MXenes*, Sc<sub>2</sub>C monolayer has a band gap of about 0.45–1.80 eV after OH, F, or O surface functionalization.<sup>[14]</sup> Moreover, it is feasible to make Sc<sub>2</sub>CO<sub>2</sub> a direct band gap semiconductor by applying an electric field or a strain.<sup>[16,17]</sup> Using first-principles calculations, it is predicted that both of Sc<sub>2</sub>CT<sub>2</sub> (*T* = F, OH) show excellent carrier mobility and thermal properties, and the thermal conductivities are higher than those of most metals and semiconducting low-dimensional materials.<sup>[8]</sup> It is also found that, by doping transition metals (Ti, V, Cr, or Mn) into Sc<sub>2</sub>CT<sub>2</sub> (*T* = OH, F, or O) structures, those TM-doped Sc<sub>2</sub>CT<sub>2</sub> systems show heterogeneous magnetic and electronic properties.<sup>[18]</sup> Thus, it is expected that semiconducting Sc<sub>2</sub>CT<sub>2</sub> (*T* = OH, F, or O) monolayer is one promising material for the design of new devices in nanoelectronics, nanophotonics, and optoelectronics. However, no studies to date have been conducted to investigate the optical properties of functionalized Sc<sub>2</sub>C monolayers. In the present study, we highlight the connection between the tunable electronic properties of Sc<sub>2</sub>CT<sub>2</sub> and their optical properties. A comprehensive research of optical characteristics is achieved through dielectric function, absorption coefficients, reflectivity, loss function, and refraction index.

\*Project supported by the Fundamental Research Funds for the Central Universities, China (Grant No. 30915014101).

†Corresponding author. E-mail: yuleidu@126.com

## 2. Computational details

The present calculations were carried out within the full-potential method with mixed basis APW+lo (FLAPW) as implemented in WIEN2k code.<sup>[19]</sup> The effects of the approximation to the exchange–correlation energy were treated by the generalized gradient approximation (GGA).<sup>[20]</sup> The muffin-tin radii ( $R_{\text{mt}}$ ) for Sc, C, O, F, and H were chosen in such a way that the spheres did not overlap. A mesh of 200  $k$ -points has been applied in the entire Brillouin zone. To obtain the total energy convergence, the plane wave cutoff parameters  $R_{\text{mt}}K_{\text{max}} = 7$ , where  $R_{\text{mt}}$  is the smallest atomic sphere radius in the unit cell and  $K_{\text{max}}$  is the magnitude of the largest  $K$  vector in the plane wave expansion. For the exceptions,  $R_{\text{mt}}K_{\text{max}}$  for  $\text{Sc}_2\text{C}(\text{OH})_2$  with short bond-length was set as 4. A vacuum space of 20 Å was introduced to avoid interactions between adjacent sheets. Atomic positions and lattice parameters were all relaxed to reach energy convergence of  $10^{-5}$ /unit cell. In this article, a perpendicular polarized light with respect to the film was applied to the two-dimensional  $\text{Sc}_2\text{C}T_2$  monolayers.

## 3. Results and discussion

The structural configurations for pristine  $\text{Sc}_2\text{C}$  and functionalized  $\text{Sc}_2\text{C}$  monolayers with OH, F, or O chemical groups have been examined by calculating the total energies of possible models, and the most stable ones are used in this article, as shown in Fig. 1. For  $\text{Sc}_2\text{C}(\text{OH})_2$  and  $\text{Sc}_2\text{CF}_2$ , the two chemical groups are located on the top of the hollow site. For  $\text{Sc}_2\text{CO}_2$ , one chemical group is located on the top of the hollow site and the other chemical group is located on the top of the C-top site. The unit cells of  $\text{Sc}_2\text{C}$ ,  $\text{Sc}_2\text{C}(\text{OH})_2$ ,  $\text{Sc}_2\text{CF}_2$ , and  $\text{Sc}_2\text{CO}_2$  have hexagonal lattice parameters of 3.31 Å, 3.31 Å, 3.29 Å, and 3.43 Å, respectively. In addition, the thermodynamic stability of the functionalized  $\text{Sc}_2\text{C}$  systems was studied by calculating the binding energy, which is defined as

$$E_{\text{for}} = E_{\text{tot}}(\text{Sc}_2\text{CT}_2) - E_{\text{tot}}(\text{Sc}_2\text{C}) - E_{\text{tot}}(T_2),$$

where  $E_{\text{tot}}(\text{Sc}_2\text{C})$  and  $E_{\text{tot}}(\text{Sc}_2\text{CT}_2)$  are the total energies of pristine and functionalized  $\text{Sc}_2\text{C}$ , and  $E_{\text{tot}}(T_2)$  is the total energy of  $\text{O}_2 + \text{H}_2$ ,  $\text{F}_2$ , and  $\text{O}_2$  for OH, F, and O terminated  $\text{Sc}_2\text{C}$  systems, respectively. The calculated binding energy is  $-11.91$  eV,  $-12.13$  eV, and  $-10.49$  eV for  $\text{Sc}_2\text{C}(\text{OH})_2$ ,  $\text{Sc}_2\text{CF}_2$ , and  $\text{Sc}_2\text{CO}_2$ , respectively. These large negative values of the binding energy reveal that the functionalized  $\text{Sc}_2\text{C}$  monolayers are extremely stable with strong bonds between terminal chemical groups and surface Sc atoms.

The band structures for  $\text{Sc}_2\text{C}$  monolayer and the functionalized monolayers are shown in Fig. 2. It can be noticed that the pristine  $\text{Sc}_2\text{C}$  monolayer exhibits metallic electrical conductivity. After surface functionalization, the  $\text{Sc}_2\text{CT}_2$  monolayers become semiconductors, and the band gaps ( $E_g$ ) are

0.44 eV, 1.07 eV, and 1.85 eV for the OH, F, and O terminated ones, respectively, which are consistent with the previous reports.<sup>[8,14]</sup> From Fig. 2, it can be seen that  $\text{Sc}_2\text{C}(\text{OH})_2$  has  $\Gamma$  (valence band maximum) to  $\Gamma$  (conduction band minimum) direct band gap, while  $\text{Sc}_2\text{CF}_2$  and  $\text{Sc}_2\text{CO}_2$  have  $\Gamma$  to  $\Gamma \rightarrow M$  and  $\Gamma$  to  $K$  indirect band gaps, respectively. Though the indirect band gaps of  $\text{Sc}_2\text{CF}_2$  and  $\text{Sc}_2\text{CO}_2$  would interrupt efficient light emission in the optical devices, the previous studies revealed that the indirect to direct band gap transition may occur under an external strain or electric field.<sup>[15–17]</sup> Stimulated by this idea, for functionalized  $\text{Sc}_2\text{C}$ , it is suitable to study its optical properties for optoelectronic applications.

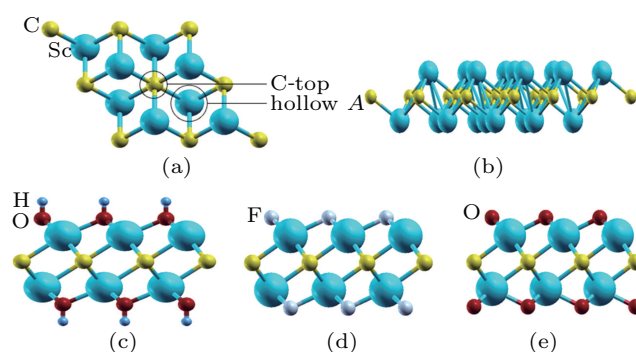


**Fig. 1.** (color online) (a) Top view and (b) side view of pristine  $\text{Sc}_2\text{C}$  monolayer, and the stable structural configurations of functionalized  $\text{Sc}_2\text{C}$  monolayers with (c) OH, (d) F, or (e) O chemical groups.

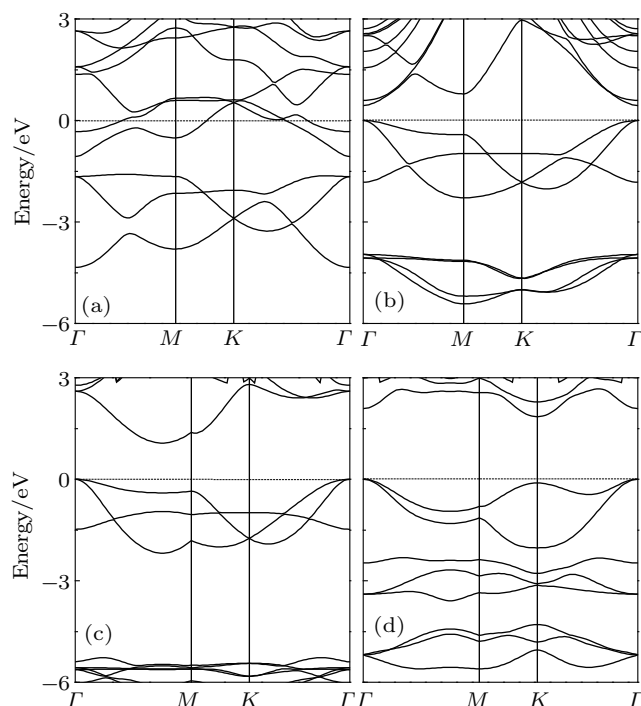


**Fig. 2.** Band structures of (a)  $\text{Sc}_2\text{C}$  monolayer and functionalized monolayers (b)  $\text{Sc}_2\text{C}(\text{OH})_2$ , (c)  $\text{Sc}_2\text{CF}_2$ , and (d)  $\text{Sc}_2\text{CO}_2$ .

To ascertain this transition of the band structures of the functionalized  $\text{Sc}_2\text{C}$  monolayers, the total and partial densities of states of pristine and functionalized  $\text{Sc}_2\text{C}$  monolayers are plotted in Fig. 3. Similar to other  $\text{MXenes}$ ,<sup>[21]</sup> the states at the Fermi level for pristine  $\text{Sc}_2\text{C}$  are mainly contributed by

Sc 3d orbital electrons, as shown in Fig. 3(a). Sc 3d and C 2p states strongly couple between  $-4.4$  eV and  $-1.5$  eV. An antibonding state forms between the coupled states and the Sc 3d states with a gap of  $0.5$  eV. The lowest-lying states from  $-10.2$  eV to  $-9.0$  eV are contributed by C 2s states. In contrast to the  $\text{Sc}_2\text{C}$  case, upon OH, F or O functionalization, the Fermi level shifts downward to the center of the gap between Sc 3d-C 2p coupled states and Sc 3d states, see Figs. 3(b)–3(d). This is the reason why functionalized  $\text{Sc}_2\text{C}$  becomes a semiconductor. Another distinguishing change is that new states are created below the Fermi level after either OH, F, or O functionalization. These new states are derived from the hybridization between Sc 3d orbitals and O 2p orbitals/F 2p orbitals. It is noteworthy that these new states are separated from the Sc 3d-C 2p coupled states with a gap  $G$  of  $1.39$  eV,  $2.93$  eV, and  $0.14$  eV for  $\text{Sc}_2\text{C}(\text{OH})_2$ ,  $\text{Sc}_2\text{CF}_2$ , and  $\text{Sc}_2\text{CO}_2$ , respectively.

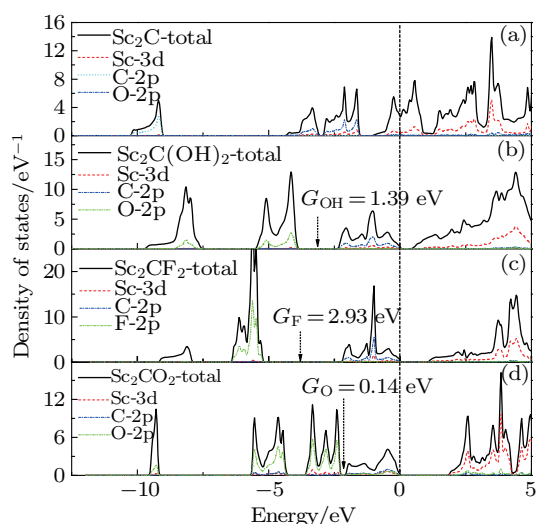


**Fig. 3.** (color online) The total and partial densities of states for (a)  $\text{Sc}_2\text{C}$ , (b)  $\text{Sc}_2\text{C}(\text{OH})_2$ , (c)  $\text{Sc}_2\text{CF}_2$ , and (d)  $\text{Sc}_2\text{CO}_2$ . The Fermi level is set to  $0$  eV.

The calculated real and imaginary parts of the dielectric function as a function of the photon energy for functionalized  $\text{Sc}_2\text{CT}_2$  ( $T = \text{OH}, \text{F}, \text{or O}$ ) monolayers are shown in Fig. 4. The imaginary part  $\varepsilon_2(\omega)$  is determined from the momentum matrix elements between the occupied and the unoccupied electronic states. From Fig. 4(a), it is clear that  $\varepsilon_2$  starts from about  $0.44$  eV,  $1.07$  eV, and  $1.85$  eV for  $\text{Sc}_2\text{C}(\text{OH})_2$ ,  $\text{Sc}_2\text{CF}_2$ , and  $\text{Sc}_2\text{CO}_2$ , respectively, corresponding to the band gap. Below  $6.0$  eV, there are two major peaks at  $2.35$  eV and  $4.31$  eV for  $\text{Sc}_2\text{C}(\text{OH})_2$ , and two major peaks appear at  $3.28$  eV and  $4.37$  eV for  $\text{Sc}_2\text{CF}_2$ . From the electronic structure, we can see that these major peaks of  $\varepsilon_2$  for  $\text{Sc}_2\text{C}(\text{OH})_2$  and  $\text{Sc}_2\text{CF}_2$  monolayers are mainly originated from the transitions from occupied Sc 3d-C 2p coupled states to unoccupied Sc 3d states. Either the O or F 2p electrons from terminated OH and F groups cannot be excited by the low-energy photons

below  $6.0$  eV. Unlike  $\text{Sc}_2\text{C}(\text{OH})_2$  and  $\text{Sc}_2\text{CF}_2$ ,  $\text{Sc}_2\text{CO}_2$  has two shoulder peaks at  $5.18$  eV and  $5.92$  eV, which are principally determined by the electronic transitions from Sc 3d-O 2p coupled states in the valence band to Sc 3d states in the conduction band. The excited O 2p orbital electrons can be ascribed to the tiny value of  $G_O$  for  $\text{Sc}_2\text{CO}_2$  with comparison to the huge value of  $G$  for  $\text{Sc}_2\text{C}(\text{OH})_2$  and  $\text{Sc}_2\text{CF}_2$  as depicted in Fig. 3. At the high-energy range (more than  $12.5$  eV),  $\varepsilon_2$  does not strongly depend on the type of functional groups and equals to  $\sim 0.5$ .

The  $\varepsilon_1(\omega)$  is obtained from imaginary part  $\varepsilon_2(\omega)$  by Kramers–Kronig transformation. The static dielectric constant  $\varepsilon_1(0)$  without any contribution from lattice vibration is equal to about  $2.93$ ,  $2.46$ , and  $2.20$  for  $\text{Sc}_2\text{C}(\text{OH})_2$ ,  $\text{Sc}_2\text{CF}_2$ , and  $\text{Sc}_2\text{CO}_2$ , respectively. The  $\varepsilon_1(0)$  shows a gap-dependent character, i.e., a wider energy gap yields a smaller  $\varepsilon_1(0)$ . This inversely proportional property could be understood within a framework of Penn model expression:<sup>[22]</sup>  $\varepsilon_1(0) \approx 1 + (\hbar\omega_p/E_g)^2$ , where  $\omega_p$  is the plasma frequency. Like  $\varepsilon_2$ , at larger photon energies,  $\varepsilon_1$  decreases monotonically with increasing photon energy and tends to present similar dielectric properties for all functionalized monolayers.

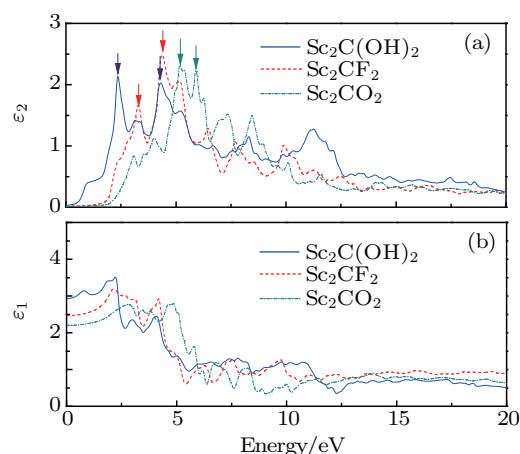


**Fig. 4.** (color online) The calculated (a) imaginary and (b) real parts of dielectric functions for  $\text{Sc}_2\text{CT}_2$  ( $T = \text{OH}, \text{F}, \text{or O}$ ).

Figures 5(a)–5(d) show the calculated energy dependences of absorption coefficient  $\alpha(\omega)$ , reflectivity  $R(\omega)$ , energy loss function  $L(\omega)$ , and refractive index  $n(\omega)$ , respectively. We should emphasize that the increase in the energy band gap from  $\text{Sc}_2\text{C}(\text{OH})_2$  to  $\text{Sc}_2\text{CF}_2$  to  $\text{Sc}_2\text{CO}_2$  manifests in the edge of the optical absorption, which is located at  $0.44$  eV,  $1.07$  eV, and  $1.85$  eV, respectively. These edges of  $\alpha(\omega)$  give the threshold for the optical transitions between the highest valence band and the lowest conduction band. The absorption coefficient shows an increasing trend at low frequency and then becomes almost constant beyond  $12.5$  eV. The optical reflectivity  $R(\omega)$  for  $\text{Sc}_2\text{C}(\text{OH})_2$ ,  $\text{Sc}_2\text{CF}_2$ , and  $\text{Sc}_2\text{CO}_2$ , as illustrated in Fig. 5(b), moderately rise and reach a maximum value

of 0.12. In the range of 0–20 eV, the reflectivity  $R(\omega)$  is always lower than 15% for either  $\text{Sc}_2\text{C}(\text{OH})_2$ ,  $\text{Sc}_2\text{CF}_2$ , or  $\text{Sc}_2\text{CO}_2$ , which indicates that functionalized  $\text{Sc}_2\text{C}$  is transparent. The energy loss function is an important factor describing the energy loss of a fast electron traversing in a material.<sup>[23]</sup> The most prominent peak in the energy-loss spectrum is identified as the plasmon peak and locates at 12.5 eV for  $\text{Sc}_2\text{C}(\text{OH})_2$ , 10.6 eV for  $\text{Sc}_2\text{CF}_2$ , and 10.2 eV for  $\text{Sc}_2\text{CO}_2$ , as shown in Fig. 5(c). These peaks correspond to the irregular edges in the reflectivity spectrum. For instance, the prominent peak of  $L(\omega)$  is at 12.5 eV for  $\text{Sc}_2\text{C}(\text{OH})_2$  corresponding to the abrupt reduction of  $R(\omega)$ , as shown in Fig. 5. The static refractive index  $n(0)$  is calculated to be 1.71 for  $\text{Sc}_2\text{C}(\text{OH})_2$ , 1.57 for  $\text{Sc}_2\text{CF}_2$ , and 1.48 for  $\text{Sc}_2\text{CO}_2$ , and we obtain the following relation between  $n(0)$  and  $\epsilon_1(0)$ :  $n(0)^2 = \epsilon_1(0)$ . The refractive index at low energy is inversely related to the band gap. Then  $n(\omega)$  reach maximum values of around 1.92 at 2.24 eV for  $\text{Sc}_2\text{C}(\text{OH})_2$ , 1.79 at 4.2 eV for  $\text{Sc}_2\text{CF}_2$ , 1.74 at 4.88 eV for  $\text{Sc}_2\text{CO}_2$ .

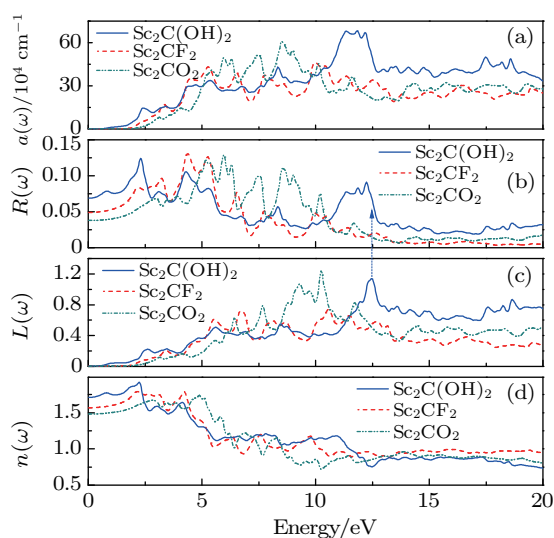


**Fig. 5.** (color online) Calculated optical parameters of  $\text{Sc}_2\text{CT}_2$  ( $T = \text{OH}$ ,  $\text{F}$ , or  $\text{O}$ ): (a) absorption coefficient/ $10^4 \text{ cm}^{-1}$ , (b) reflectivity, (c) energy loss function, and (d) refractive index.

In general, with the increase of the energy gap from OH to F then to O terminated  $\text{Sc}_2\text{C}$ , the dielectric function (both real and imaginary parts) as well as other optical parameters will shift toward red, and the peak increases obviously in the low-energy range, as illustrated in Figs. 4 and 5. Due to this feature, we find strong dependent behaviors in optical properties with respect to the type of chemical groups. From the electronic structure shown in Figs. 2 and 3, in the low-energy region, it can be seen that the phonon adsorption essentially is dominated by the Sc 3d orbital, whereas the O 2p and F 2p orbital electrons from the terminated groups could not be excited. For instance, the O 2p valence electrons in  $\text{Sc}_2\text{CO}_2$  monolayer will transfer to Sc 3d conduction bands only when the phonon energy is higher than 5.18 eV.

The difference in optical properties among OH, F, and O functionalized  $\text{Sc}_2\text{C}$  is mainly ascribed to the different electronic coupling between terminated groups and surface Sc atomic layer. As mentioned above, the conductivity for pristine  $\text{Sc}_2\text{C}$  originates from the unpaired 3d electrons of Sc at the Fermi level. When the  $\text{Sc}_2\text{C}$  surface is terminated with higher electronegative chemical groups, the electrons transfer from  $[\text{Sc}_2\text{C}]$  layers to the attached groups. The number of free electrons decreases by coupling with O 2p electrons or F 2p electrons, the Fermi level shifts upward and the functionalized  $\text{Sc}_2\text{C}$  monolayers turn out to be semiconducting as exhibited in Fig. 3. By using Bader charge analysis,<sup>[24]</sup> the effective atomic charges of  $\text{Sc}_2\text{CT}_2$  ( $T = \text{OH}$ ,  $\text{F}$ , or  $\text{O}$ ) were calculated, and the ionic formulas are  $[\text{Sc}_2^{1.73+}\text{C}^{2.05-}]^{1.4+}[\text{O}^{1.31-}\text{H}^{0.53+}]_2^{0.7-}$ ,  $[\text{Sc}_2^{1.81+}\text{C}^{2.02-}]^{1.6+}\text{F}_2^{0.8-}$ , and  $[\text{Sc}^{1.76+}\text{C}^{1.30-}\text{Sc}^{1.91+}]^{2.36+}\text{O}^{1.12-}\text{O}^{1.24-}$ . It is clear that there is a close association between the band gap size and the number of transfer electrons. Consequently, an open band gap is a result of surface functionalization, and the gap size can vary depending on the interaction between chemical groups and  $\text{Sc}_2\text{C}$  surface with a gap opening of up to 0.44–1.55 eV. This dependent changing of  $\text{Sc}_2\text{C}$  structure due to functionalization would open a way to tune the electronic and optical properties of *MXene*. Presently, the study keystone of functionalization is how to modulate the type of surface groups. According to the experimental results, the surface functionalization is highly sensitive to the synthesis method.<sup>[25–29]</sup> For the HF etching method, *MXenes* are mostly covered by OH groups with few F and O terminations present.<sup>[25,26]</sup> By using a milder etchant, LiF dissolved in 6 M HCl, the O termination is a relatively major component with a low content of OH and F terminal groups.<sup>[27]</sup> Moreover, it was considered that high-temperature annealing could cause the conversion of OH to O terminations, and hence the O terminated ones generally can be obtained.<sup>[26,28]</sup> Though some researches of surface functionalization have been done, a more complete understanding of these interesting 2D materials would promote the development for practical applications.

## 4. Conclusion

The electronic and optical properties for two-dimensional  $\text{Sc}_2\text{C}$  with OH, F, or O chemical groups were investigated using first-principles calculation. The chemical groups are stably adsorbed on the  $\text{Sc}_2\text{C}$  surface by interacting with Sc 3d orbital electrons. After surface functionalization, the electronic structures are changed and the  $\text{Sc}_2\text{C}$  monolayer transforms from metallic to semiconductor with a gap opening of up to 0.44–1.55 eV. The dielectric function (both real and imaginary parts) as well as other optical parameters shift to red, and the peak increases obviously in the low-energy range with the increase of the energy gap. The comprehensive theoretical study of the

optical properties opens up a scope for designing the tunable optoelectronic devices.

## References

- [1] Anasori B, Xie Y, Beidaghi M, Lu J, Hosler B C, Hultman L, Kent P R C, Gogotsi Y and Barsoum M W 2015 *ACS Nano* **9** 9507
- [2] Shein I R and Ivanovskii A L 2013 *Micro Nano Lett.* **8** 59
- [3] Naguib M, Kurtoglu M, Presser V, Lu J, Niu J, Heon M, Hultman L, Gogotsi Y and Barsoum M W 2011 *Adv. Mater.* **23** 4248
- [4] Naguib M, Mashtalir O, Carle J, Presser V, Lu J, Hultman L, Gogotsi Y and Barsoum M W 2012 *ACS Nano* **6** 1322
- [5] Naguib M and Gogotsi Y 2015 *Acc. Chem. Res.* **48** 128
- [6] Harris K J, Bugnet M, Naguib M, Barsoum M W and Goward G R 2015 *J. Phys. Chem. C* **119** 13713
- [7] Xie Y and Kent P R C 2013 *Phys. Rev. B* **87** 235441
- [8] Zha X H, Luo K, Li Q, Huang Q, He J, Wen X and Du S 2015 *Europhys. Lett.* **111** 26007
- [9] Zhang X, Ma Z, Zhao X, Tang Q and Zhou Z 2015 *J. Mater. Chem. A* **3** 4960
- [10] Berdiyrov G R 2015 *Appl. Surf. Sci.* **359** 153
- [11] Berdiyrov G R 2015 *Europhys. Lett.* **111** 67002
- [12] Zha X H, Zhou J, Zhou Y, Huang Q, He J, Francisco J S, Luo K and Du S 2016 *Nanoscale* **8** 6110
- [13] Gan L Y, Zhao Y J, Huang D and Schwingenschlögl U 2013 *Phys. Rev. B* **87** 245307
- [14] Khazaei M, Arai M, Sasaki T, Chung C Y, Venkataramanan N S, Estili M, Sakka Y and Kawazoe Y 2013 *Adv. Funct. Mater.* **23** 2185
- [15] Yu X, Cheng J, Liu Z, Li Q, Li W, Yang X and Xiao B 2015 *RSC Adv.* **5** 30438
- [16] Lee Y, Cho S B and Chung Y C 2014 *ACS Appl. Mater. Interfaces* **6** 14724
- [17] Lee Y, Hwang Y, Cho S B and Chung Y C 2014 *Phys. Chem. Chem. Phys.* **16** 26273
- [18] Yang J, Luo X, Zhang S and Chen L 2016 *Phys. Chem. Chem. Phys.* **18** 12914
- [19] Blaha P, Schwarz K, Madsen G K H, Kvasnicka D and Luitz J 2001 *WIEN2k: An Augmented Plane Wave Plus Local Orbitals Program for Calculating Crystal Properties* (Austria: Vienna University of Technology)
- [20] Perdew J P, Burke K and Ernzerhof M 1996 *Phys. Rev. Lett.* **77** 3865
- [21] Kurtoglu M and Naguib M 2012 *MRS Commun.* **2** 133
- [22] Penn D R 1962 *Phys. Rev. B* **128** 2093
- [23] Nozieres P and Pines D 1959 *Phys. Rev.* **113** 1254
- [24] Bader R F W 1990 *Atom in Molecules: A Quantum Theory* (New York: Oxford University Press) p. 155
- [25] Halim J, Cook K M, Naguib M, Eklund P, Gogotsi Y, Rosen J and Barsoum M W 2016 *Appl. Surf. Sci.* **362** 406
- [26] Xie Y, Naguib M, Mochalin V N, Barsoum M W, Gogotsi Y, Yu X, Nam K W, Yang X Q, Kolesnikov A I and Kent P R C 2014 *J. Am. Chem. Soc.* **136** 6385
- [27] Hope M A, Forse A C, Griffith K J, Lukatskaya M R, Ghidui M, Gogotsi Y and Grey C P 2016 *Phys. Chem. Chem. Phys.* **18** 1583
- [28] Karlsson L H, Birch J, Halim J, Barsoum M W and Persson P O Å 2015 *Nano Lett.* **15** 4955
- [29] Halim J, Lukatskaya M R, Cook K, Lu J, Smith C R, May S J, Hultman L, Gogotsi Y, Eklund P and Barsoum M W 2014 *Chem. Mater.* **26** 2374